J. Fluid Mech. (1987), *vol.* 183, *pp.* 163–173
Printed in Great Britain

Observations of dispersion of entrained fluid in the self-preserving region of a turbulent jet

By D. JOSEPH SHLIEN

Mechanical Engineering Department, University of Nebraska – Lincoln, Lincoln, NE 68588, USA

(Received 13 April 1986 and in revised form 10 March 1987)

Ambient fluid of a submerged water jet was continuously tagged with fluorescent dye at a point outside the turbulent region (at 33 jet nozzle diameters from the jet exit). This made it possible to follow the tagged entrained fluid to 73 jet diameters downstream of the exit, a distance unattainable by other methods. The dispersion of the tagged fluid in a plane containing the jet axis and the tagging source was observed and recorded using photography and simple digital image-processing techniques. Most of the entrainment activity appeared to be the result of engulfment by the large-scale structures over an axial distance of $\pm 1.7B$ from the source where B is the half-peak velocity radius. The entrained fluid crossed the jet centreline within a downstream distance of $\Delta x = 1.5B$.

Downstream of the entrainment region, the spread rate of the tagged entrained fluid was close to that of the turbulent jet fluid. However, the peak mean concentration of the tagged entrained fluid was located near the $r/x = 0.1$ line closest to the tagging source and shifted very slowly towards the jet centreline. A self-preserving distribution of the mean concentration appears to have been approached after a distance of $6B$ downstream from the tagging source but further verification is needed owing to experimental uncertainties.

A small fraction of the tagged entrained fluid was found on the side of the jet remote from the tagging source. On rare occurrences, tagged entrained fluid was observed at the interface most remote from the source.

1. Introduction

In order to predict and enhance either combustion or the dispersion of pollutants in fluids, it is essential to understand the process of entrainment, a major phenomenon of free turbulent shear flows. Yet there are very few direct observations or measurements of entrainment. This is due to the difficulty of performing such measurements with conventional (pointwise) instruments such as hot-wire anemometers, laser-Doppler anemometers or resistance thermometers. Until recently, flow visualization which simultaneously yields properties in a field, mainly provided qualitative data. With the development of digital image processing, images from flow visualization experiments could be digitized and quantitative data extracted. These data would not normally be accessible with conventional measuring techniques. Here quantitative data will be presented on the entrained fluid dispersion in an axisymmetric turbulent jet.

The author is unaware of any previous direct study of the dispersion of entrained fluid in a jet. Works closely related to this subject are those in which the turbulent (jet) fluid was tagged by scalars such as temperature, chemical composition or solid

particles and the dilution of the scalar was measured. Such measurements were pioneered by Corrsin (1943) and Hinze & Van der Hegge Zijnen (1951). More recent works are by Becker, Hottel & Williams (1967), Antonia, Prabhu & Stephenson (1975), Shaughnessy & Morton (1977), Birch *et al.* (1978), Chevray & Tutu (1978), and Dahm & Dimotakis (1985) to give just a sample of various types of related experiments. There are also several early attempts at measuring dispersion of a scalar contaminant inside turbulent jets: notably by Corrsin & Uberoi (1951) and by Hinze & Van der Hegge Zijnen (1951). In these experiments heat was used to tag the fluid in a small region but due to the rapid dispersion, the temperature difference could only be measured with reasonable accuracy over small distances (less than an integral scale of the turbulence).

Our ability to predict the dispersion in shear flows is severely limited by the lack of theory. This situation is well summarized in the review paper by Hunt (1985) who expressed the need for more measurements.

There are only a few direct measurements of entrainment velocity, the pioneering work being by Ricou & Spalding (1961). Hill (1972) improved upon this method.

Techniques related to those used here have been presented by Koochesfahani & Dimotakis (1984) to measure the concentration of mixed fluid in a plane mixing layer. They used flow-visualization techniques with real-time data acquisition along a straight line perpendicular to the flow. Only one fluid of the two-stream mixing layer was dyed.

Here are presented the first measurements of the dispersion of entrained fluid from a small source external to the turbulent field. The techniques used will be described in the next section, followed by observations of the dispersion by short-exposure photographs, and then by long-exposure photographs.

2. Equipment and procedures

2.1. *Flow facility*

The flow facility consisted of a large water tank, 1.8 m diameter by 2.7 m high having four glass viewing windows 0.9 m by 1.5 m high as shown in figure 1. The constant-head tank was fed through a circular diffuser. Screens near the nozzle entrance improved velocity uniformity and reduced the turbulence level. An end plate of diameter equal to 40 nozzle diameters was used to assure consistency with other investigations. A constant-head tank at the exit of the large tank maintained the main water tank level constant during the experiment. Considerable care was taken to maintain isothermal conditions of all the water used. The maximum ratio of the jet half-peak velocity width, B, to the tank diameter in the region of observation was 0.13, resulting in a small effect due to the walls of the tank. A screened plenum above the tank exit (see figure 1) reduced adverse effects of the fluid exiting the tank and effects of the tank bottom. The jet Reynolds number was 12.3×10^3 and the nozzle exit diameter d, was 1.52 cm.

2.2. *Tagging of entrained fluid*

The entraining fluid passing the point $(x/d, r/d) = (33.3, 12.0)$ was continuously tagged by radially injecting 20 p.p.m. of rhodamine B fluorescent dye at approximately the estimated average entrainment velocity through a 30 cm long, 10 mm diameter tube. This velocity was computed using equation (14) in Ricou & Spalding (1961). Here x and r are the axial and radial coordinates for the jet, respectively. The

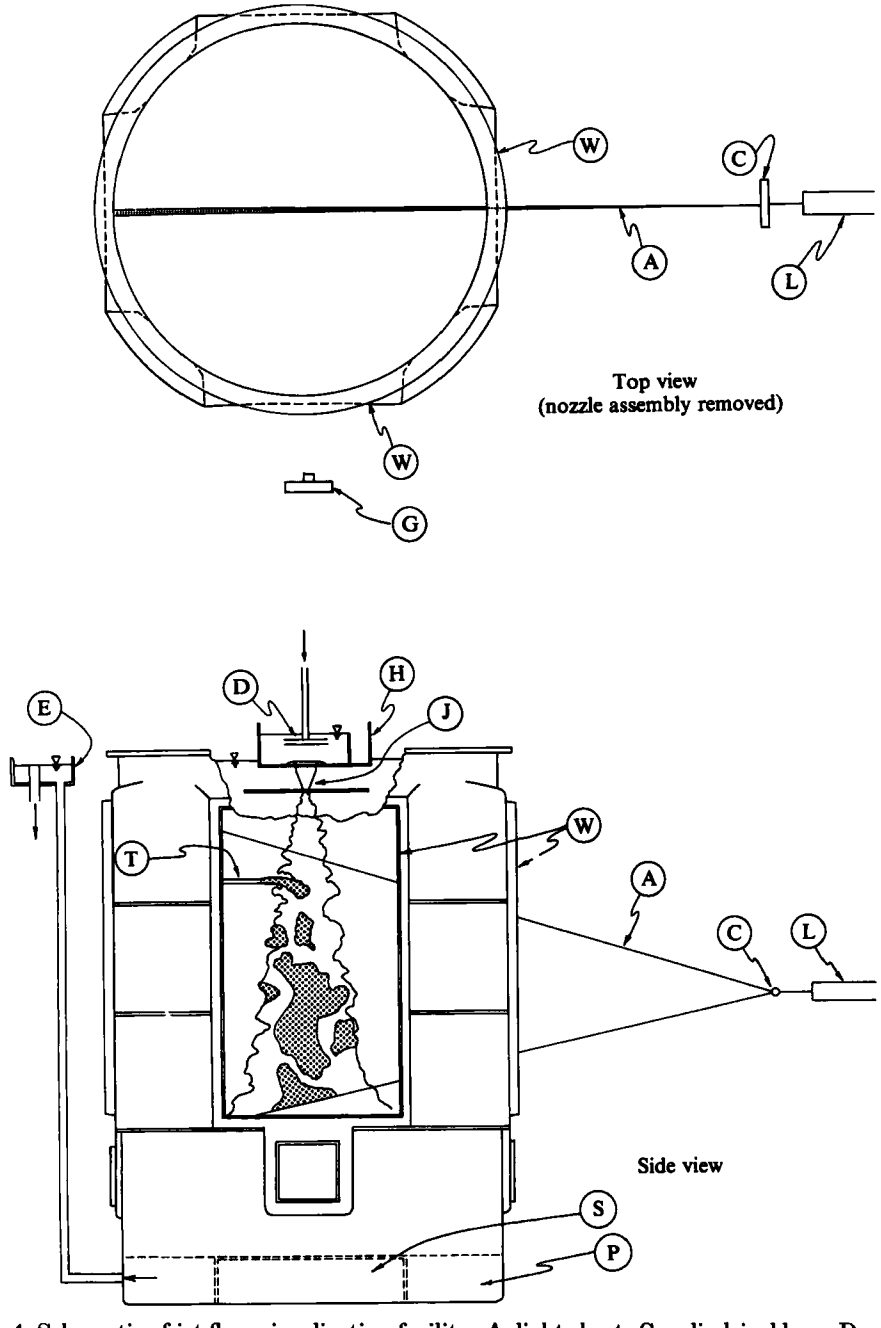

FIGURE 1. Schematic of jet flow visualization facility: A, light sheet; C, cylindrical lens; D, circular diffuser; E, outlet constant-head assembly; G, camera; H, constant-head supply tank; J, jet nozzle; L, laser; P, exit plenum; S, screened enclosure; T, tube for dyed entraining fluid source; W, glass window.

relatively large tube diameter and high initial concentration were necessary to obtain a sufficiently high mean dye concentration far downstream. The tube diameter nevertheless was 0.10 of the local half-peak velocity width and thus should not have introduced large errors.

2.3. *Field illumination*

The fluorescent dye at the concentrations used was barely visible under normal illumination. However, it fluoresced and thus became highly visible when illuminated by light of appropriate wavelength. Using a cylindrical lens to expand the beam from a 5W argon laser into a sheet through the jet axis, a cross-section of the fluid entrained in the jet was obtained. For the mean concentration measurements reported here, the light sheet was not thinned (thickness about 10 mm) to obtain additional averaging.

2.4. *Photographic and image-processing techniques*

The cross-section described in the previous paragraph was photographed with a standard 35 mm camera and the resulting negatives were digitized. The digital image-processing system consisted of an Eikonix 78/99 image digitizing camera of resolution 1728 × 2048 pixels (picture elements) and was interfaced with a PDP 11/34 digital computer. To save storage space, the images were digitized to a depth of 128 (7 bits) grey levels. The digitized and processed images were displayed using a Vectrix VX384 colour graphics unit and a display of resolution 672 × 480 pixels.

The digitized image consists of a two-dimensional array of grey levels, each grey level corresponding to a concentration of dye at a point in the light sheet. Under normal circumstances, the dye concentration C, can be computed from the grey level G, by:

$$C = k(G - G_0)^b, \tag{1}$$

where k and b are constants obtained by calibration and G_0 represents the background grey level. However, it was found that an exposure time of 100 s was required to obtain reasonably smooth (spatially) average concentrations. For such long exposure times, photographic film behaves irregularly: the opacity of the exposed and developed film depends upon both the time duration of exposure and the light intensity separately rather than simply upon their product. This behaviour is called reciprocity failure. This separate dependence is such that if the film exposure time to an object of given brightness is doubled, the opacity of the area of film affected will be less than doubled. In the context of the present experiment, consider two regions which have the same average dye concentration: region 1 of concentration 80 for 10 s and concentration 0 for 90 s while the concentration of region 2 is 8 for the 100 s exposure time. The effective exposure time of region 1 will be only 10 s as compared with 100 s for region 2 (since the film is assumed to be unaffected by a zero concentration). Thus reciprocity failure will result in region 2 having an apparently lower mean concentration than region 1.

The net result of reciprocity failure is that the constant b in (1) depends upon the effective exposure time duration (which in turn, depends upon the fluid particle residence time at the point, i.e. the fluid velocity there). The exponent b increases with increasing exposure time (or in sensitometry terms, the value of γ decreases with increasing exposure times). Thus an upper bound on b was found by calibration with three known dye concentrations for exposure time durations of 100 s. This resulted in $b = 1.7$.

Another difficulty with using photographic film to record the flow-visualization image results from light being reflected from the back surface of the film during its

exposure. This process, called halation, causes a relatively weak halo at the edge of an intense exposure and is observable in the digitized images.

The validity of the results to be presented were verified by averaging the images of eight short-exposure photographs of the distribution of tagged entrained fluid. Using short exposures eliminated reciprocity failure and halation effects at the cost of a very limited averaging sample.

Six small lights outside of the far tank window opposite the camera provided spatial reference points on the film. An initial photograph of a plumbline suspended from the jet nozzle as well as a lengthscale provided the means to determine spatial coordinates of the digitized image. After a set of flow-visualization photographs of the experiment were taken, dye was mixed to a uniform concentration in the tank and then photographed under the identical illumination as in the flow-visualization pictures. This provided a reference photographic negative to compensate for both non-uniform illumination of the flow field and of the negative when it was being digitized. A no. 30 Kodak Wratten gelatin filter placed in front of the camera lens attenuated scattered laser light while passing the fluoresced light.

3. Observations

3.1. *Short-time-exposure photographs*

The short-time-exposure photographs in figure 2 (plate 1) have been selected for their diversity in distributions of entrained fluid. (For these photos the laser light sheet was thinned to a thickness of several millimetres.) In figure 2(*b*) and especially figure 2(*c*) most of the tagged entrained fluid is found on the side of the jet closest to the entrained fluid source. Furthermore, the tagged entrained fluid can be seen to be mixed with the jet fluid right out to the interface. Very little tagged entrained fluid is seen near the interface remote from the source in figure 2(*b*) and (*c*), while in figure 2(*a*), some of the tagged entrained fluid is found in that region. In all four photographs the tagged entrained fluid is seen to have crossed the jet centre-line. Observation of the dye emerging from the tagging tube confirms that the dye injection rate was reasonable.

It should be noted that the apparent regions of isolated dyed fluid cannot be truly isolated but must be 'attached' to the main body of jet fluid outside the plane of observation (although in some cases the attachment may be so tenuous as to be considered detached, see Chevray 1984; Omer & Chevray 1982). Also to be noted are the dark regions inside the jet. These represent untagged entrained fluid, but they are not necessarily irrotational, because the diffusivity of vorticity is several orders of magnitude greater than that of the dye used in these experiments.

3.2. *Long-time averages*

The mean concentration distribution of entrained fluid originating from the localized source can be estimated from long-time-exposure photographs corresponding to those of figure 2 (but without the green dye). A photo of the digitized image in 128 uniformly spaced grey levels is presented in figure 3(*a*) (plate 2). By using a spectrum of 128 false colours to replace the grey levels, considerably more detail is visible (figure 3*b*). In order to differentiate between contour levels more clearly, a single colour is assigned to ten adjacent grey levels, starting with levels 1 to 10 (figure 3*c*). However, because it is also desirable to distinguish between each of the lowest grey levels, ten different colours are also assigned to the lowest ten grey levels (figure 3*d*). Note that it is the relative grey levels G, that are displayed in figure 3 rather than

the mean concentration of the tagged entrained fluid C. This accentuates the lower concentration levels (see equation (1)).

The jet centreline (thick white line) is superimposed upon the digitized images and the pairs of lines on either side of the centreline indicate the $r/x = 0.1$ and 0.2 locations. ($r/x = 0.1$ approximately corresponds to the location of the half-peak mean axial velocity or half-peak mean jet fluid concentration, while $r/x = 0.2$ corresponds to the 5% peak values. The outer region of the visible portion of dyed jet fluid lies just outside this $r/x = 0.2$ surface.) The axial distance (in jet exit diameters) from the jet exit is indicated near the right-hand side of the photos. The source of the tagged fluid is located at $(x/d, r/x) = (33.3, 0.36)$, well inside the non-turbulent flow region. At $x \approx 45d$, the dye distribution appears to be distorted – this is caused by an extraneous reflection of light scattered from the dye source tube (also visible in figure 2).

In the absence of molecular diffusion, the probability of finding tagged entrained fluid at a point in the flow field is proportional to the mean concentration at that point. Thus under ideal circumstances, figure 3 in conjunction with (1) would give contours of constant probability. However because of the existence of molecular diffusion and because the exponent b in (1) cannot be determined reliably, this interpretation must be considered very approximate. In subsequent discussions, b will be assumed to equal 1.7 and $G_0 = 6$ for estimates of probabilities. It is also to be noted that the maximum grey level (or mean concentration or probability) should be found at the tagging source exit; but in these photographs the maximum is somewhat removed from that position. This was caused by the absorption of some of the illumination by the higher dye concentration near the source which shaded the dyed fluid behind it.

In the photographs of figure 3, the lower concentration levels are represented by dark blues while higher concentrations correspond to longer wavelength colours. The entire range of grey levels are shown in sequence at the right-hand side of each photo. In addition, in figure 3(d) the lowest ten grey levels are also shown on the left-hand side of the photograph.

The averaging time (film exposure duration) appears to be reasonable, although increasing this time would smooth out the irregularities in the outer regions of the jet. From figure 3(d), it is apparent that the probability of finding tagged entrained fluid just at the visible jet edge closest to the source is of order 0.05% (one grey level above the background level of yellow, $G_0 = 6$). This probability increased to about 0.3% within a radial distance $\Delta r = 0.02x$. At the far side of the jet (most remote from the source) the increase to a probability of 0.3% was considerably more gradual requiring a seven-fold Δr. (Note that due to halation effects, there is some doubt as to the radial extent of the observed tagged entrained fluid.) These contours closely followed the lines of constant r/x after an initial development distance of $2B$ to $3B$ downstream. The probability of the tagged entrained fluid crossing the jet centreline becomes 0.3% ($G = 10$) within $\Delta x = 1.5B$ from the source, and increased to 2.5% ($G = 20$) after $\Delta x = 2.5B$. It subsequently remained close to that level for most of the remaining observed region. The peak probability was located at $r = 0.12x$ at section $x = 37d$, and slowly shifted towards the centreline so that by $x = 73d$, the peak was located at $r = 0.07x$ with little change observed from $x = 55d$. The reader is cautioned that the values of the probability quoted here are very approximate, mainly due to the reciprocity-failure difficulties. Errors may be as large as an order of magnitude in the outer region of the jet. Work is at present underway to obtain more accurate measurements.

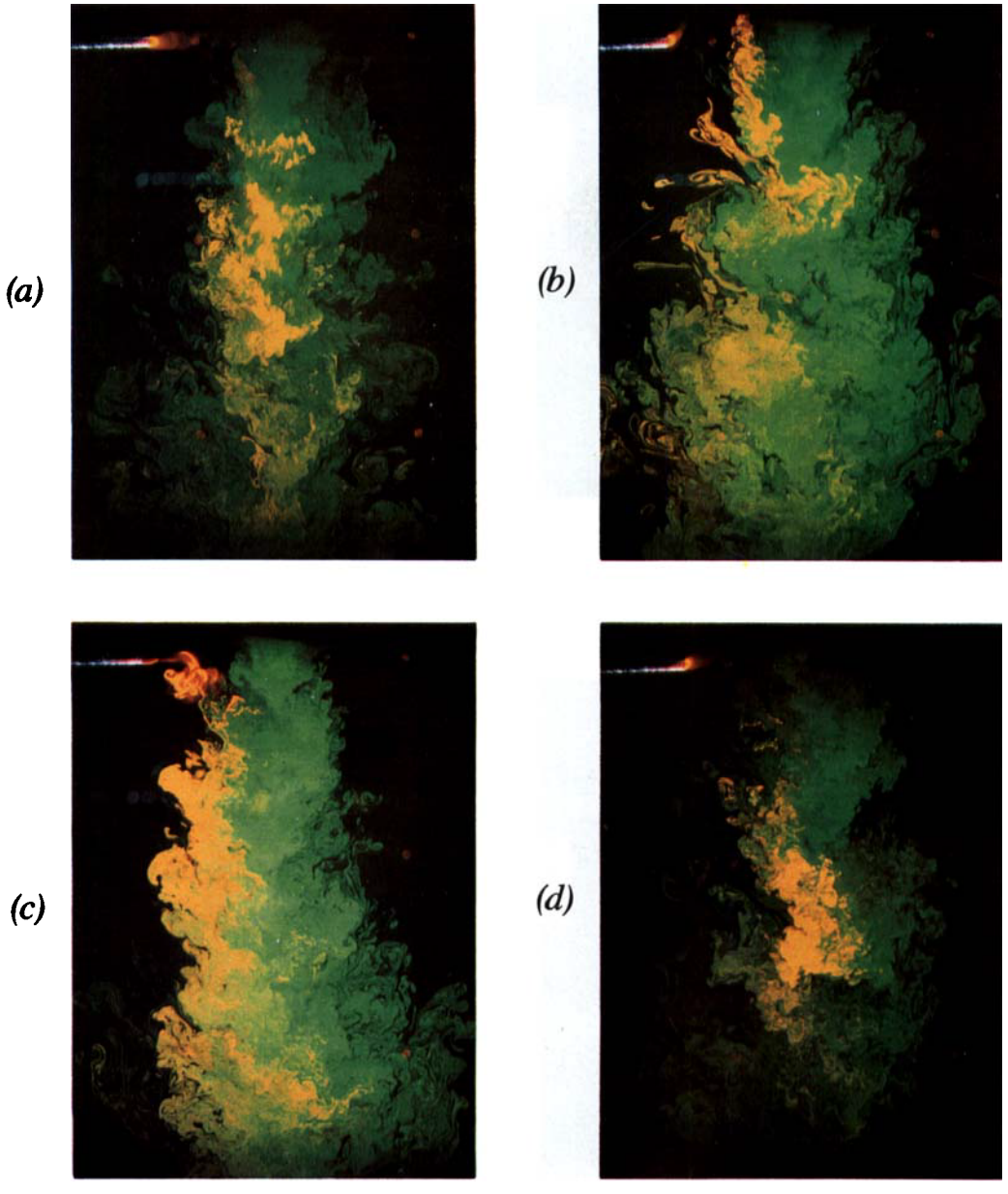

FIGURE 2. Short-time photographic exposure of a cross-section containing the jet axis. Flow is from top of photograph, downwards. Three pairs of reference points (small orange circles all of which are visible in (*a*) and (*d*)) are at x/d = 33, 54, and 67. The green dye tags the fluid which emerged from the jet nozzle while the other colour dye marks the fluid entrained from ambient fluid passing the point (x/d, r/x) = (33, 0.36). The second dye is actually red but photographs yellow except for the region near the source. For these photographs, the light sheet was thinned to about 3 mm.

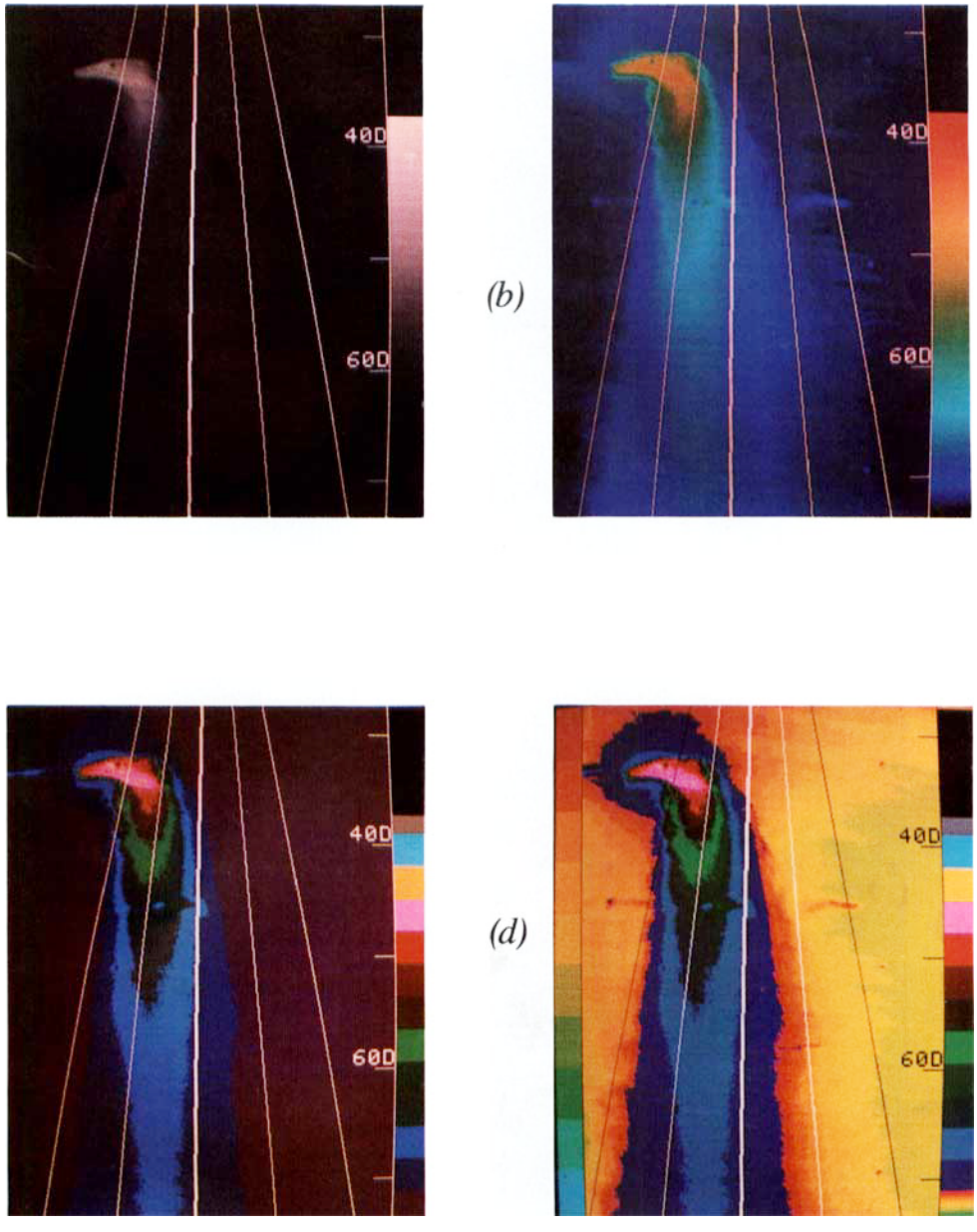

FIGURE 3. Long-time photographic exposure of entrained fluid. The thick vertical line indicates the jet centreline and the pairs of lines on either side of the centreline indicate $r/x = 0.1$ and 0.2 locations. The axial distance from the jet nozzle exit is given at the right-hand side of the photos, in number of jet exit diameters. (*a*) 128 grey levels in black and white; (*b*) substitution of a spectrum of 128 false colours in place of the grey levels; (*c*) 13 false colours, emphasizing contour levels; and (*d*) same as (*c*) but with the lowest 10 levels in different colours.

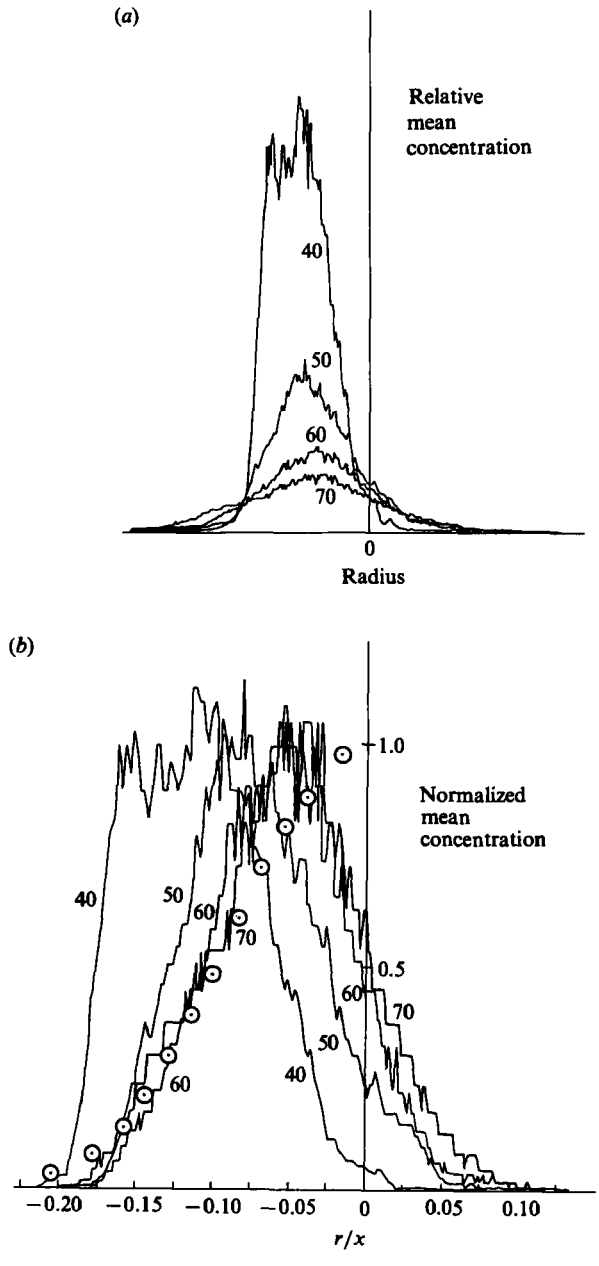

FIGURE 4. Mean concentration profiles. (*a*) Unnormalized. Numbers next to the curves indicate the x/d position. (*b*) Normalized to verify self-similarity. The concentrations are normalized with the peak values while the radial position is normalized with the distance from the jet exit to the profile under consideration. Data points are of the jet fluid concentration from Chevray & Tutu (1978).

The shift in the peak is also apparent in the plot of mean concentration against radial coordinate for four axial positions (figure 4*a*). It is clear from this graph that only a small fraction of the entrained fluid has dispersed across the centre plane. To check for self-preservation, the mean concentrations have been normalized by the peak value of each section and the radial coordinate r was normalized by the axial

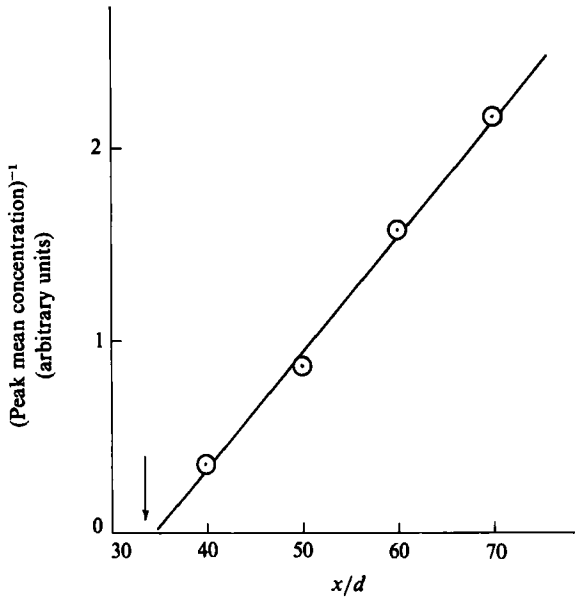

FIGURE 5. Inverse of peak concentration as a function of downstream position for the data of figure 4. The arrow points to the actual axial position of the source of entrained fluid.

position from the jet exit, x (figure 4*b*). No apparent source correction was applied. A self-preserving form appears to have been approached by $x = 60d$, although there is a slight systematic deviation between the $x = 60d$ and $x = 70d$ profiles for $r > -0.02x$, i.e. on the side of the profiles remote from the source. This may indicate a slow dispersion towards 'filling' the far side of the turbulent jet with entrained tagged fluid. The mean concentration profile of tagged entrained fluid is close to that of the jet fluid for $r < -0.06x$ and $x > 60d$, which might indicate that the entrained fluid is almost completely mixed there. However, when the photographs of figure 2 are examined, it can be seen (especially figure 2*d*) that this is not the case.

The inverse of the peak values of mean concentration used in the normalization of figure 4(*a*) are plotted in figure 5. A linear variation of the inverse peak value was also obtained for the jet mean centreline velocity and for jet mean concentration at the centreline from similarity consideration.

4. Discussion

To verify that the gross features of the mean concentration distribution obtained by long-time-exposure photographs are reasonable in the light of uncertainties introduced by reciprocity failure and halation, the instantaneous concentration distribution obtained from eight short-exposure photographs were averaged. Within the considerable scatter which resulted from such a small sample, it was observed that the tagged fluid did indeed cross the jet centreline close to the source and that the peak concentration remained at a fixed radial distance from the jet axis.

The tagged entraining fluid is drawn deeply into the turbulent jet: to the $r = 0.1x$ line almost immediately and to the jet axis within an axial distance of $1.5B$. The mechanism of such a rapid transport of fluid must be by engulfment at the upstream

side of the large-scale structures. This engulfment process was suggested by Bevilaqua & Lykoudis (1977) and observed by Anderson, LaRue & Libby (1979) for example, and also observed by the author in flow-visualization motion pictures in a plane air jet (Shlien & Hussain 1982) as well as in motion pictures corresponding to figure 2. The engulfment was observed to extend beyond the jet centreline. When engulfed fluid approaches the central region of the jet, the relatively high axial jet velocity there transports it downstream and it is observed to cross the centreline somewhat below the source; however it still is expected to have been transported to that position by the original large-scale structure. Most of the entrainment activity from the tagging source takes place within an axial distance of $\pm 1.7B$ from the source (i.e. for $x < 40d$). The observed size of the jet large-scale structures is of order $3.5B$ (Shlien & Hussain 1982).

Beyond the entrainment region for the tagged fluid ($x > 40d$), the entrained fluid spreads with the turbulent jet fluid (see figure $3d$ where contour features are observed to spread with the $r/x =$ constant lines). In fact, it is speculated that if the jet fluid were tagged at a point in the neighbourhood of $x = 30d$ and $r = 0.1x$, the concentration distribution of the tagged fluid for $x > 40d$ would be similar to that observed for the tagged entrained fluid observed here. (This could define an entry distance or apparent source position for the entrainment.) The rate of this dispersion as detected by downstream changes is relatively slow due to the small radial and angular velocity components compared with the axial velocity component. Asymptotically, it is expected that the tagged entrained fluid will become completely mixed with the jet fluid and thus its concentration distribution will be the same as that for the jet fluid. However this trend is so slow that it cannot be detected in these observations with the exception of the peak concentration position; it moves towards the jet axis rather than spreading radially with the jet fluid.

The mean concentration distribution of the tagged entrained fluid appears to have approached a self-preserving form by $x > 60d$ ($\Delta x = 6B$). However, if it is assumed that eventually the tagged entrained fluid will become completely mixed with the jet fluid (fluid which originated in the jet nozzle), then clearly the asymptotic mean concentration distribution of the tagged entrained fluid must approach that of the turbulent jet fluid. Measurements over a considerably larger range of distance are required to verify this.

5. Conclusions

Most of the entrainment activity takes place within an axial distance $\pm 1.7B$ from the source. The main mechanism is by engulfment by the large-scale structures which carry volumes of ambient fluid into the turbulent jet fluid and, at times, transport the ambient fluid across the jet centreline. Beyond the entrainment region, the tagged entrained fluid disperses very slowly with respect to the spreading jet: (i) the peak mean concentration of tagged entrained fluid shifted from $(x, r) = (37d, 0.12x)$ to $(73d, 0.07x)$ with little change in the radial position observed from $x = 55d$ and (ii) the mean concentration distribution of the tagged entrained fluid may have approached a self-preserving form by $x > 60d$. Verification of these conclusions is necessary owing to uncertainties resulting from reciprocity failure.

The short-exposure photographs of figure 2, the mean concentration distributions, and the observation that the mean concentration gradient on the side of source is much greater than that on the remote side of the source are all consistent with an

entrainment model in which the large-scale structures draw tongues of ambient fluid to a position in the jet near $r = 0.13x$ with random penetrations beyond the jet centreline. Plans are underway to build upon this concept to predict the mean concentration distribution resulting from entrainment.

Measurements of intermittency in the circular jet normally give an intermittency of unity on and near the jet axis. This would seem to imply that no non-turbulent fluid crosses the jet axis; yet it is plainly seen in the measurements presented here that entrained fluid not only crosses the jet axis but crosses it within a relatively short downstream distance from the source of ambient fluid. There is no evidence of contradiction here, the dyed fluid visible in the jet was originally non-turbulent but this fluid may be turbulent by the time it crosses the jet axis since vorticity diffuses much more rapidly than the dye (large Schmidt number). However, as a result of the author's observations of the engulfment of ambient fluid (in other experiments), he believes that the intermittency on the axis may indeed be less than unity. The measurements of intermittency presented in the literature are, to the author's knowledge, all limited in their resolution of narrow regions (short convection time) of non-turbulent fluid. Thus it may be that the intermittency on the jet axis is somewhat below unity but undetected by conventional measurement methods due to the rapid passage of relatively narrow regions of non-turbulent fluid past the sensing transducer.

The author wishes to acknowledge the valuable discussions with Stanley Kleis who helped formulate aspects of this research. Suggestions from the editor and referees considerably improved this paper. Partial support from the Engineering Research Center and from the University Research Council is gratefully acknowledged. In addition, several undergraduate students helped in the computer programming and in setting up the experiments. This work is dedicated to the memory of S. Corrsin.

REFERENCES

Anderson, P., LaRue, J. C. & Libby, P. A. 1979 Preferential entrainment in a two-dimensional turbulent jet in a moving stream. *Phys. Fluids* **22**, 1857–1861.

Antonia, R. A., Prabhu, A. & Stephenson, S. E. 1975 Conditionally sampled measurements in a heated turbulent jet. *J. Fluid Mech.* **72**, 455–480.

Becker, H. A., Hottel, H. C. & Williams, G. C. 1967 The nozzle-fluid concentration field of the round, turbulent, free jet. *J. Fluid Mech.* **30**, 285–303.

Bevilaqua, P. M. & Lykoudis, P. S. 1977 Some observations on the mechanism of entrainment. *AIAA J.* **15**, 1194–1196.

Birch, A. D., Brown, D. R., Dodson, M. G. & Thomas, J. R. 1978 The turbulent concentration field of a methane jet. *J. Fluid Mech.* **88**, 431–449.

Chevray, R. & Tutu, N. K. 1978 Intermittency and preferential transport of heat in a round jet. *J. Fluid Mech.* **88**, 133–160.

Chevray, R. 1984 Entrainment in turbulent flows: mechanisms and implications. In *Turbulence and Chaotic Phenomena in Fluids* (ed. T. Tatsumi), pp. 365–369. Elsevier.

Corrsin, S. 1943 Investigation of flow in an axially symmetric heated jet of air. *NACA Wartime Rep.* W-94.

Corrsin, S. & Uberoi, M. S. 1951 Spectra and diffusion in a round turbulent jet. *NACA Rep.* 1040.

Dahm, W. J. A. & Dimotakis, P. E. 1985 Measurements of entrainment and mixing in turbulent jets. *AIAA paper* 85-0056.

Hill, B. J. 1972 Measurement of local entrainment rate in the initial region of axisymmetric turbulent air jets. *J. Fluid Mech.* **51**, 773–779.

HINZE, J. O. & VAN DER HEGGE ZIJNEN, B. G. 1951 *General Discussion on Heat Transfer*, p. 188. IMechE, London.

HUNT, J. C. R. 1985 Turbulent diffusion from sources in complex flows. *Ann. Rev. Fluid Mech.* **17**, 447–486.

KOOCHESFAHANI, M. M. & DIMOTAKIS, P. E. 1984 Laser induced fluorescence measurements of concentration in a plane mixing layer. *AIAA paper* 84-0198.

OMER, S. & CHEVRAY, R. 1982 Entrainment mechanisms in turbulent flows. *Proc. 9th US Natl Congress of Appl. Mech.*

RICOU, F. P. & SPALDING, D. B. 1961 Measurements of entrainment by axisymmetrical turbulent jets. *J. Fluid Mech.* **11**, 21–33.

SHAUGHNESSY, E. J. & MORTON, J. B. 1977 Laser light-scattering measurements of particle concentration in a turbulent jet. *J. Fluid Mech.* **80**, 129–148.

SHLIEN, D. J. & HUSSAIN, A. K. M. F. 1982 Visualization of the entraining flow in the self-preserving region of a turbulent plane jet. *J. Flow Vis. Soc. of Japan* **2**, 587–593.

Note added in proof. With respect to figure 2, preliminary measurements from over 100 short-exposure photographs indicate that the peak mean concentration at $x = 70d$ is approximately 1/100 of the peak concentration of dye near the tagging source.